Encapsulation of Anionic Dye Molecules by a Swelling Fluoromica through Intercalation of Cationic Polyelectrolytes

Hideo Hata, Yoji Kobayashi, and Thomas E. Mallouk*

Department of Chemistry, The Pennsylvania State University, University Park, Pennsylvania 16802

Received August 13, 2006. Revised Manuscript Received October 15, 2006

To develop a novel layered host material with the ability to encapsulate anionic substances, the intercalation of three cationic polyelectrolytes into synthetic sodium fluortetrasilisic mica (Na-TSM) was investigated. With polyethylenimine (PEI) and poly(allylamine hydrochloride) (PAH), the conformation of the intercalated polycation and its ability to accommodate anionic guests depended on its state of protonation. The quaternary ammonium polycation poly(diallyldimethylammonium) (PDDA), which had the lowest charge density of the three polymers studied, adopted a coiled conformation within the anionic host at both high and low pH, resulting in an excess of cationic sites within the interlayer of the polysilicate. Powder X-ray diffraction patterns and adsorption isotherms showed two different stages of PDDA intercalation with different adsorption free energies. Atomic force microscopy images showed that the PDDA−clay nanocomposites maintained the shape of the original nanosheets, indicating the successful conversion of the lamellar host into a 2D material with anion exchange capacity. The anion-accepting ability of these nanocomposites was quantified by studying the encapsulation of a bulky anionic blue dye as a function of the loading of PDDA. From dehydration and X-ray powder diffraction experiments, it was concluded that the dye−polyelectrolyte−clay nanocomposites possessed two kinds of interlayer galleries, and the anionic dye was site-selectively intercalated into hydrated galleries in which PDDA strands were coiled.

Introduction

Functional materials are often made by the synergistic combination of organic and inorganic components. Over the past decade, the trend in this field has been shifting toward more sophisticated multifunctional nanomaterials, many of which utilize the very high surface-to-volume ratio of layered inorganic hosts.[1−4] These hosts include polysilicates,[2] layered double hydroxides (LDHs),[2] layered perovskites,[4] layered transition metal oxides,[4] metal phosphates,[2] metal chalcogenides, graphitic carbon, and other lamellar materials.[2] Intercalation reactions convert these hosts to ordered inorganic−organic assemblies with structures controlled by host−guest and guest−guest interactions, leading to a rich variety of properties and applications. With the prominent exception of LDHs, however, almost all layered host materials, as well as many open framework hosts, such as zeolites, have an anionic framework, meaning that they can accept only cationic or basic guests. This severely limits the range of organic molecules and polymers that can be incorporated into such nanocomposite materials. Although LDHs have a positive layer charge, there are also several important limitations of LDH hosts. LDHs typically have a high layer charge density, resulting in a strong electrostatic interaction between the layers and interlayer anions. This causes difficulty in exfoliating the solid, which usually involves insertion of wedgelike organic anions to weaken the interlayer attraction, followed by dispersion in organic or aqueous solvents.[5−8] LDHs are additionally basic and easily contaminated by atmospheric CO_2, which leads to intercalated CO_3^{2-} ions. Therefore, LDHs are less than ideal hosts for many applications of porous pillared materials.[9]

The principle of the alternate adsorption using oppositely charged colloidal particles was pioneered by Iler in 1966.[10] Our group later reported the alternate adsorption of multiply charged transition metal ions and diphosphonic acids to make well-ordered metal−organic films.[11] In the early 1990s, Decher et al. extended this concept to the sequential adsorption of oppositely charged polyelectrolytes.[12] At the heart of each of these procedures is the overcompensation of surface charge by the next adsorbed layer; this effect both limits the adsorption to a single layer and inverts the surface

* Corresponding author. E-mail: tom@chem.psu.edu.

(1) Sanchez, C.; Soler-Illia, G. J. A.; Robit, F.; Lalot, T.; Mayer, C. R.; Cabuil, V. *Chem. Mater.* **2001**, *13*, 3061−3083.
(2) Auerbach, S. M.; Carrado, K. A.; Dutta, S. M. *Handbook of Layered Materials*; Marcel Dekker Inc.: New York, 2004.
(3) Decher, G.; Schlenoff, J. B. *Multilayer Thin Films*; Wiley−VCH Verlag GmbH & Co. KGaA: Weinheim, 2003.
(4) Ogawa, M.; Kuroda, K. *Chem. Rev.* **1995**, *95*, 399−438.
(5) (a) Adachi-Pagano, M.; Forano, C.; Besse, J. P. *Chem. Commun.* **2000**, 91−92. (b) Leroux, F.; Adachi-Pagano, M.; Intissar, M.; Chauvière, S.; Forano, C.; Besse, J. P. *J. Mater. Chem.* **2001**, *11*, 105−112.
(6) (a) Hibino, T.; Jones, W. J. *Mater. Chem.* **2001**, *11*, 1321−1323. (b) Hibino, T. *Chem. Mater.* **2004**, *16*, 5482−5488. (c) Hibino, T.; Kobayashi, M. *J. Mater. Chem.* **2005**, *15*, 653−656.
(7) O'Learly, S.; O'Hare, D.; Seeley, G. *Chem. Commun.* **2002**, 1506−1507.
(8) Li, L.; Ma, R.; Ebina, Y.; Iyi, N.; Sasaki, T. *Chem. Mater.* **2005**, *17*, 4386−4391.
(9) Ohtsuka, K. *Chem. Mater.* **1997**, *9*, 2039−2050.
(10) Iler, R. K. *J. Colloid Interface Sci.* **1966**, *21*, 569−594.
(11) (a) Lee, H.; Kepley, L.; Hong, H.-G.; Mallouk, T. E. *J. Am. Chem. Soc.* **1988**, *110*, 618−620. (b) Cao, G.; Hong, H.-G.; Mallouk, T. E. *Acc. Chem. Res.* **1992**, *25*, 420−427. (c) Yang, H.; Aoki, K.; Hong, H. G.; Sackett, D.; Arendt, M.; Yau, S. L.; Bell, C.; Mallouk, T. E. *J. Am. Chem. Soc.* **1993**, *115*, 11855−11862. (d) Fang, M.; Kaschak, D. M.; Sutorik, A. C.; Mallouk, T. E. *J. Am. Chem. Soc.* **1997**, *119*, 12184−12191.

10.1021/cm061908c CCC: $37.00
Published on Web 12/07/2006

charge for the next adsorption step.[3,12] This sequential electrostatic adsorption method, which is now called the layer-by-layer (LBL) technique, has attracted the interest of many researchers because of its experimental simplicity. In general, the sequential deposition of anionic and cationic polymers results in "fuzzy" nanostructures in which adjacent oppositely charged layers strongly interpenetrate.[12b] However, the incorporation of exfoliated lamellar colloids into the LBL scheme[13−15] allows one to make well stratified "lasagna" structures, which can have minimal layer interpenetration.[14b] LBL films of this type typically include anionic sheet colloids such as clays,[3,13,15] α-$Zr(HPO_4)_2 \cdot H_2O$,[14] layer perovskites,[16] $Ti_{1-\delta}O_2$ ($\delta \approx 0.09$),[17] and $HTiNbO_5$,[18] although analogous structures incorporating cationic LDH sheets have also been reported.[19]

In at least one case, the LBL method has been used to incorporate anionic dye molecules into an assembly of anionic sheets by interposing polycation layers.[14d] On the basis of this result, we hypothesized that it should be possible to overcompensate the negative surface charge of polysilicate nanosheets by intercalation of coiled polycations, effectively creating a new kind of cationic host. As far as we know, there have only been a few reports of the intercalation of polyelectrolytes into layered materials.[20−24] Darder et al. investigated the intercalation of Chitosan into montmorillonite and the ability of the resulting composite to incorporate small anions such as NO_3^-, CH_3COO^-, Cl^-, SO_3^{2-}, $Cr_2O_7^{2-}$, and $Fe(CN)_6^{3-}$.[22] In that study, Chitosan was found to intercalate as a bilayer of extended polymer chains at high concentrations, creating an excess of cationic sites.

Scheme 1. Reactions of Na-TSM To Form a Monolayer of Intercalated Polycation (Step 1), and a Coiled Polycation That Overcompensates the Layer Charge (Step 2). Large Anions Are Exchanged for Intercalated Small Anions in Step 3

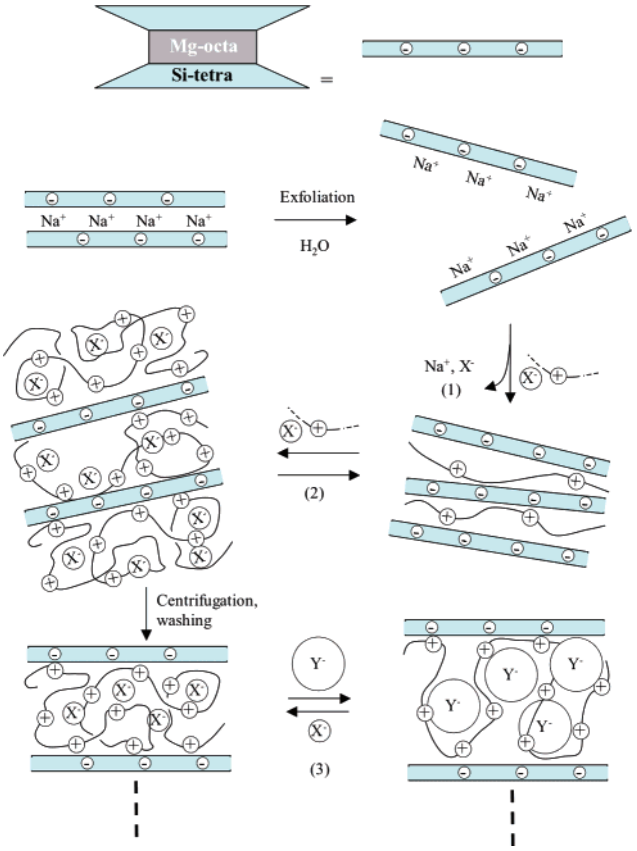

To incorporate large anionic guests (such as typical dye molecules), the polymer chain should have the flexibility to coil and overcompensate the negative charge of the sheets, as illustrated in Scheme 1. Lower charge density polycations are preferred, because of their ability to bind low charge density, hydrophobic anions more strongly than smaller anions. We find that with high charge density polycations, a simple intercalation reaction (step 1 in Scheme 1) occurs to give a dense nanocomposite in which the polycation is extended and intercalated as a monolayer. With the low charge density polymers, additional polymer is incorporated in a coiled conformation (step 2) to overcompensate the layer charge. Small anions intercalated in this process can be replaced by larger, low charge density anions (step 3).

In the first part of this study, we investigated the intercalation of several cationic polyelectrolytes with different charge densities into an exfoliated synthetic fluoromica. In the second part, we studied the encapsulation of a bulky acidic dye (Figure 1, FD & C Blue 1) by the restacked polycation/fluoromica nanocomposite under different conditions. The resulting materials were evaluated by means of structural, compositional, spectroscopic, and morphological analyses.

Experimental Section

Materials. Sodium fluortetrasilisic mica with the chemical formula $Na_{0.66}Mg_{2.68}(Si_{3.98}Al_{0.02})O_{10.02}F_{1.96}$ and a cation exchange

(12) (a) Decher, G.; Hong, J.-D.; Schmitt, J. *Thin Solid Films* **1992**, *210/211*, 504. (b) Decher, G. *Science* **1997**, *277*, 1232−1237.
(13) (a) Kleinfeld, E. R.; Ferguson, G. S. *Science* **1994**, *265*, 370−373. (b) Kleinfeld, E. R.; Ferguson, G. S. *Chem. Mater.* **1995**, *7*, 2327−2331.
(14) (a) Keller, S. W.; Kim, H.-N.; Mallouk, T. E. *J. Am. Chem. Soc.* **1994**, *116*, 8817−8818. (b) Kaschak, D. M.; Mallouk, T. E. *J. Am. Chem. Soc.* **1996**, *118*, 4222−4224. (c) Kim, H.-N.; Keller, S. W.; Mallouk, T. E.; Schmitt, J.; Decher, G. *Chem. Mater.* **1997**, *9*, 1414−1421. (d) Kaschak, D. M.; Lean, J. T.; Waraksa, C. C.; Saupe, G. B.; Usami, H.; Mallouk, T. E. *J. Am Chem. Soc.* **1999**, *121*, 3435−3445.
(15) (a) Lvov, Y.; Ariga, K.; Ichinose, I.; Kunitake, T. *Langmuir* **1996**, *12*, 3038−3044. (b) Kotov, N. A.; Haraszti, T.; Turi, L.; Zavala, G.; Geer, R. E.; Dékány, I.; Fendler, J. H. *J. Am. Chem. Soc.* **1997**, *119*, 6821−6832. (c) Kotov, N. A.; Magonov, S.; Tropsha, E. *Chem. Mater.* **1998**, *10*, 886−895. (d) van Duffel, B.; Schoonheydt, R. A.; Grim, C. P. M.; De Schryver, F. C. *Langmuir* **1999**, *15*, 7520−7529. (e) Kim, D. W.; Blumstein, A.; Kumar, J.; Tripathy, S. K. *Chem. Mater.* **2001**, *13*, 243−246.
(16) (a) Schaak, R. E.; Mallouk, T. E. *Chem. Mater.* **2000**, *12*, 2513−2516. (b) Schaak, R. E.; Mallouk, T. E. *Chem. Mater.* **2000**, *12*, 3427−2424.
(17) (a) Sasaki, T.; Ebina, Y.; Watanabe, M.; Decher, G. *Chem. Commun.* **2000**, 2163−2164. (b) Sasaki, T.; Ebina, Y.; Tanaka, T.; Harada, M.; Watanabe, M.; Decher, G. *Chem. Mater.* **2001**, *13*, 4661−4667.
(18) Fang, M.; Kim, C. H.; Saupe, G. B.; Kim, H. N.; Waraksa, C. C.; Miwa, T.; Fujishima, A.; Mallouk, T. E. *Chem. Mater.* **1999**, *11*, 1526−1532.
(19) Li, L.; Ma, R.; Ebina, Y.; Iyi, N.; Sasaki, T. *Chem. Mater.* **2005**, *17*, 4386−4391.
(20) Ruehrwein, R. A.; Ward, D. W. *Soil Sci.* **1952**, *73*, 485−492.
(21) Breen, C. *Appl. Clay Sci.* **1999**, *15*, 187−219.
(22) (a) Darder, M.; Colilla, M.; Ruiz-Hitzky, E. *Chem. Mater.* **2003**, *15*, 3744−3780. (b) Darder, M.; Colilla, M.; Ruiz-Hitzky, E. *Appl. Clay Sci.* **2005**, *28*, 199−208.
(23) Darder, M.; López-Blanco, M.; Aranda, P.; Leroux, F.; Ruiz-Hitzky, E. *Chem. Mater.* **2005**, *17*, 1969−1977.
(24) JP Patent 3219971.

Table 1. Analytical Data for PDDA/Na-TSM and B1/PDDA/Na-TSM Nanocomposites

B1/PDDA/Na-TSM initial molar ratio	amount of PDDA adsorbed/mmol/100 g clay	amount of B1 adsorbed/mmol/100 g clay	PDDA/Na-TSM molar ratio	B1/PDDA molar ratio
1/0/1		0.50		
1/1/1	93.6	5.00	0.78	5.33×10^{-2}
1/2/1	112	9.11	1.02	7.44×10^{-2}
1/3/1	142	11.7	1.18	8.27×10^{-2}
1/5/1	153	16.2	1.27	10.7×10^{-2}
1/10/1	163	18.4	1.36	11.3×10^{-2}
1/5/1(K-FM)	2.31	0.57		24.7×10^{-2}

capacity (CEC) of 120 mequiv/100 g (ME-100, CO-OP Chemicals) was used as the host material. Hereafter, this sodium fluortetrasilisic mica is abbreviated as Na-TSM. Na-TSM is a synthetic 2:1-type layered silicate formed by a unique intercalation reaction of talc with Na_2SiF_6.[25] Synthetic unexpandable potassium fluoromica ($KMg_3AlSi_3O_{10}F_2$, abbreviated as K-FM) was purchased from Topy Ind. Co. High molecular weight poly(diallyldimethylammonium chloride) (PDDA) (M_W < 100 000) was purchased from Sigma-Aldrich as a 35.0 wt % aqueous solution. Poly(allylamine hydrochloride) (M_W = 15 000, abbreviated as PAH) and polyethylenimine (M_W = 25 000, abbreviated as PEI) were purchased from Sigma-Aldrich. For the electrostatic deposition experiments, poly(4-styrenesulfonic acid sodium salt) (PSS, M_W < 75 000) and poly(diallyldimethylammonium chloride) (PDDA, MW = 200 000−350 000) were purchased from Sigma-Aldrich as aqueous solutions. FD & C Blue No. 1 (Brilliant Blue FCF, abbreviated as B1) was purchased from Kishi Kasei Co., Ltd. (Yokohama). Water was deionized using a Nanopure water purification system. All of these compounds were used as received.

Intercalation of Cationic Polyelectrolytes into F-Micas. In the intercalation of cationic polyelectrolytes, Na-TSM (0.75 g) was added to 74.25 g of water, and the suspension was stirred for 1 day at room temperature to ensure that the Na-TSM was adequately exfoliated. An aqueous solution of a cationic polyelectrolyte (25.0 g) was then added, and the suspension was vigorously agitated for 1 day at 298 K. Because PEI is not soluble in water, it was first stirred for 2 h before adding it to the Na-TSM suspension. For pH adjustment, 10 N NaOH and 5 N HCl aqueous solutions were used. The content of polyelectrolyte in the suspension varied: 0.9 (1/1), 2.7 (1/3), 4.5 (1/5), and 9.0 (1/10) mmol for PEI and PAH and 0.09 (1/0.1), 0.27 (1/0.3), 0.45 (1/0.5), 0.9 (1/1), 1.8 (1/2), 2.7 (1/3), 4.5 (1/5), 9.0 (1/10), and 18.0 (1/20) mmol for PDDA. The numbers enclosed in parentheses indicate the initial ratio of the CEC of Na-TSM to the equivalents of polyelectrolyte. After the reaction, the suspension was centrifuged, and the resultant product was washed twice with 100 g of water to remove excess polymer. Finally, the sample was dried at 333 K for 1 or 2 days and ground to a powder. The nanocomposites obtained in this way are designated as PDDA/Na-TSM (*n*), PAH/Na-TSM (*n*), and PEI/Na-TSM (*n*), respectively, where *n* denotes the initial equivalent ratio of the polyelectrolyte to the CEC of Na-TSM. Table 1 shows the amounts of PDDA adsorbed onto Na-TSM calculated from carbon analysis, as well as the ratio of adsorbed PDDA to the CEC.

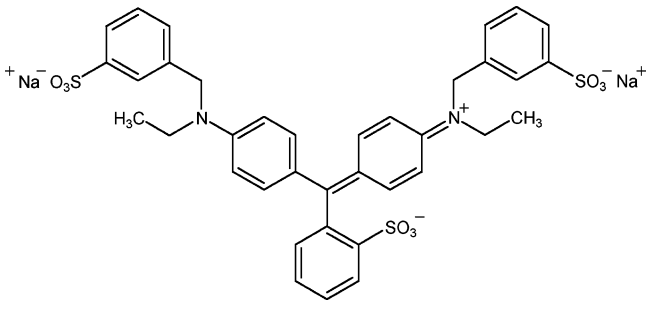

Figure 1. Structure of FD & C Blue No. 1 (B1).

Encapsulation of Acidic Dye into Polyelectrolyte/Na-TSM Nanocomposites. The encapsulation of B1 by PDDA/Na-TSM was carried out by the following method. Na-TSM (0.75 g) was added to 74.25 g of water, and the suspension was stirred for 1 day at room temperature. Next, 25.0 g of an aqueous solution containing 0, 0.9, 1.8, 2.7, 4.5, or 9.0 mmol PDDA was added to the Na-TSM suspension, and the suspension was vigorously agitated for 1 day at 298 K. The suspension was then centrifuged, and the remaining product was washed twice with 100 g of water. Water was added to the wet nanocomposite to a total weight of 75.0 g, and this suspension was added to 25.0 g of an aqueous solution containing 0.9 mmol of B1, which is an equimolar amount to the CEC of the Na-TSM used. The suspension was vigorously stirred for 1 day at room temperature, followed by centrifugation and washing three times with water. The blue colored product was dried at 333 K for 1 or 2 days and ground to a powder. The products obtained were designated as B1/PDDA/Na-TSM (*n*), respectively, where *n* again indicates the initial molar ratio polyelectrolyte to the CEC of Na-TSM.

Dehydration of the Samples for XRD Measurements. The polyelectrolyte−Na-TSM nanocomposites samples were dehydrated at 393 K for 24 h. To avoid rehydration in the atmosphere, the samples were removed from the oven and analyzed by XRD immediately.

Instrumentation. X-ray powder diffraction (XRD) patterns were obtained with a Philips X'Pert MPD diffractometer (monochromated Cu Kα_1 (λ = 0.154053 nm) radiation). Nitrogen Brunauer−Emmet−Teller (BET) surface area measurements were performed by using a Micromeritics ASAP 2010 instrument. Samples were preheated at 393 K for 3 h under 10^{-2} Torr prior to surface area measurements. Infrared spectra were recorded on a Digilab FTS 700 IR spectrometer. UV−vis absorption spectra were obtained on Hewlett-Packard 8452A diode array spectrophotometer. A Digital Instruments Nanoscope IIIA atomic force microscope (AFM) system was used to investigate the morphology of samples. AFM images were collected in tapping mode with silicon tip cantilevers with a force constant of 20 N cm^{-1}. Sample preparation for AFM was conducted as follows: A colloidal suspension of each sample (the solids content varied between 0.002 and 0.02 wt %) was shaken for 1 h before LBL adsorption. Si(001) wafers (1 cm^2) were cleaned in piranha solution (3:7 30.0% H_2O_2:98.0% H_2SO_4), which formed a 0.15−0.2 nm SiO_2 layer. *(Caution: Piranha solution is corrosive and can react violently with organic compounds, so special care should be taken when handling it.)* The substrate was washed with a copious amount of water and dried in a N_2 gas flow. Next, the clean substrate was placed in a 20 mM PDDA (MW = 200 000−350 000) aqueous solution for 20 min, washed vigorously with water, and dried in a N_2 gas flow. The wafer was then immersed in a 10 mM aqueous PSS solution for 20 min. This negatively charged substrate was used for the deposition of PDDA/Na-TSM

(25) (a) Tateyama, H.; Nishimura, S.; Tsunematsu, K.; Jinnai, K.; Adachi, Y.; Kimura, M. *Clays Clay Miner.* **1992**, *40*, 180−185. (b) Tateyama, H.; Tsunematsu, K.; Noma, H.; Adachi, Y.; Takeuchi, H.; Kohyama, N. *J. Am. Ceram. Soc.* **1996**, *79*, 3321−3324.

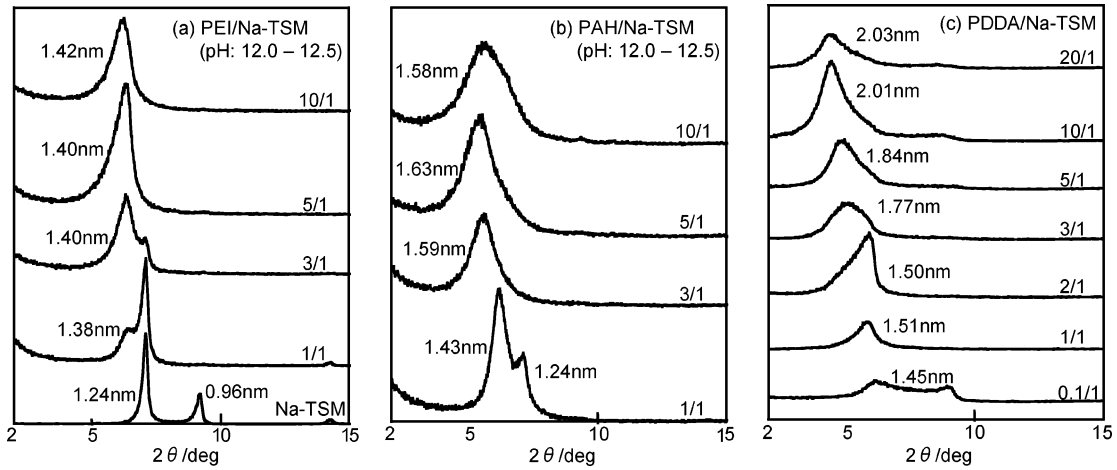

Figure 2. XRD patterns of (a) original Na-TSM and PEI/Na-TSM = 1/1, 3/1, 5/1, and 10/1 intercalated at pH 12.0−12.5, (b) PAH/Na-TSM = 1/1, 3/1, 5/1, and 10/1 intercalated at pH 12.0−12.5, and (c) PDDA/Na-TSM = 0.1/1, 1/1, 2/1, 3/1, 5/1, 10/1, and 20/1.

nanocomposites. Elemental analysis for C, H, and N was performed by Atlantic Microlabs, Inc., Norcross, GA.

Results and Discussion

Intercalation of Cationic Polyelectrolytes into Na-TSM. The goal of this part of the study was to invert the layer charge of the Na-fluortetrasilisic mica (Na-TSM) through intercalation of a cationic polyelectrolyte while preserving the morphology of the nanosheets. Cationic polyelectrolytes with three different cationic groups (PEI, PAH, and PDDA) were studied. PAH and PEI are weak base polyelectrolytes, and Shiratori et al. have found that the thickness of PAH layers adsorbed onto anionic substrates can vary with the pH of the solution.[27] Therefore, PEI and PAH were intercalated into the mica layers under both high (12.0−12.5) and low (3.0−3.5) pH conditions.

Figure 2 shows XRD patterns of the original Na-TSM, PEI, and PAH/Na-TSM composites obtained at high pH, and PDDA/Na-TSM, as a function of the initial equivalent ratio, *n*, of polyelectrolyte to Na-TSM. It is known that Na-TSM has two different kinds of interlayers, only one of which retains water molecules under ambient conditions,[26] so peaks due to phases with and without intercalated water were observed at *d*-spacings of 1.24 and 0.96 nm, respectively (Figure 2a). After dehydration of Na-TSM at 393 K for 24 h, the peak due to the hydrated layers disappeared, leaving only the 0.96 nm peak. Based on this, the basal spacing of the silicate layers was taken to be 0.96 nm.

In the PEI system at pH 12.0−12.5 (Figure 2a), when the concentration of polymer was kept low (between $n = 1$ and 3), an intercalated phase with a layer spacing of 1.40 nm was obtained in addition to residual hydrated Na-TSM (1.24 nm). At higher polymer concentrations ($n = 5$ or 10), the Na-TSM phase disappeared, but the basal spacing did not change significantly, indicating that the conformation of PEI in the interlayer did not change. When the reaction was done at low pH, the 1.40 nm intercalated phase was observed at $n = 1$, and again no significant peak shift occurred as the loading increased. Taking the thickness of the silicate layer as 0.96 nm, the expansion of interlayer space is 0.44 nm, corresponding to a single-layer extended (rather than coiled) conformation for intercalated PEI.

For PAH intercalation at high pH (Figure 2b), similar behavior was observed at $n = 1$, but at higher concentration the layer spacing of the intercalated phase increased to ca. 1.60 nm. This suggests some coiling of the polymer chains to fill a 0.6 nm interlayer gallery. When PAH was intercalated at low pH, the basal spacing increased to 1.46 nm at $n = 1$, but did not increase further up to $n = 10$. This behavior was similar to that of PEI at low pH. It suggests that at low pH, the high charge density amine polymers adopt an extended conformation and intercalate as a single layer between the silicate sheets.

Qualitatively different behavior was found for PDDA, which is a lower charge density, pH-insensitive quaternary ammonium polycation. In the XRD patterns (Figure 2c), the basal spacing steadily increased up to ca. 2.00 nm as *n* was increased from 0.1 to 10. This indicates that the PDDA chains within the interlayer adopt a successively more coiled conformation as the loading increases. The same trend was observed at low and high pH, consistent with the pH independence of the charge density of PDDA.

The diffraction peak broadens, especially in the case of relatively high loading of polycations. The increased width indicates that the size of the crystalline domains along the stacking axis decreases after the intercalation. The shapes of the peaks are asymmetric, especially with PDDA/Na-TSM intercalation compounds, indicating that there are multiple phases with a range of lattice spacings in these composites.

Thermodynamics of PDDA Intercalation into Na-TSM. Figure 3 shows the adsorption isotherm of PDDA into Na-TSM at 298 K. The amount of PDDA intercalated and the equilibrium concentration of polymer in the supernatant solution were calculated from elemental analysis (C, H, N) of the solid. In the Giles classification of solution adsorption isotherms,[28] this isotherm is classified as an H curve, which is a special case of the L curve (Langmuir type) and indicates

(26) (a) Tateyama, H.; Noma, H.; Nishimura, S.; Adachi, Y.; Ooi, M.; Urabe, K. *Clays Clay Miner.* **1998**, *46*, 245−255. (b) Inoue, K.; Tateyama, H.; Noma, H.; Nishimura, S. *Clay Sci.* **2001**, *11*, 391−404. (c) Yang, J. H.; Han, Y. S.; Choy, J. H.; Tateyama, H. *J. Mater. Chem.* **2001**, *11*, 1305−1312. (d) Imai, Y.; Nishimura, S.; Abe, E.; Tateyama, H.; Abiko, A.; Yamaguchi, A.; Aoyama, T.; Taguchi, H. *Chem. Mater.* **2002**, *14*, 477−479.

(27) Shiratori, S. S.; Rubner, M. F. *Macromolecules* **2000**, *33*, 4213−4219.

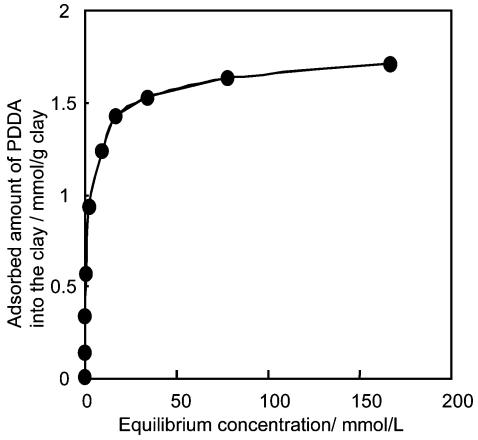

Figure 3. Adsorption isotherm of PDDA on Na-TSM, in aqueous dispersions at 298 K.

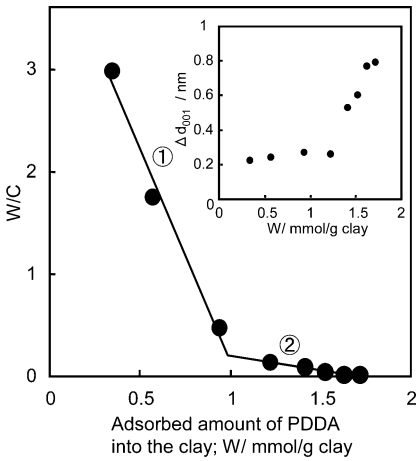

Figure 4. Scatchard plot derived from the adsorption isotherm data in Figure 3. The inset shows a Δd_{001} (differential *d*-spacing before and after intercalation of PDDA) as a function of actual adsorbed amount of PDDA.

high affinity between solute and adsorbent. From this result, PDDA should form a monolayer on the interlayer surface of Na-TSM. To linearize the Langmuir eq 1,[29] the Scatchard form, eq 2,[30] was used.

$$W = aW_sC/(1 + aC) \quad (1)$$

$$W/C = aW_s - aW \quad (2)$$

Here, W is the amount of PDDA adsorbed, C is the equilibrium concentration of PDDA, W_s is the saturated adsorbed amount of PDDA, and a is the adsorption equilibrium constant. Figure 4 shows the Scatchard plot obtained from the experimental data. In this plot, a change in slope is observed at $W \approx 0.99$ mmol/g. Because the slope of the plot corresponds to $-a$, the abrupt change in slope indicates that the adsorption behavior of PDDA changes at this point. Before and after this point, the a values were calculated to be 4.15×10^3 and 2.72×10^2 mol^{-1} L, respectively. The standard free energy of adsorption can be calculated form the a values using eq 3:

$$\Delta G^\circ_{ads} = -RT \ln K \quad (3)$$

Here, R is the gas constant, T is the adsorption temperature, and $K = (a\rho/4)^2$ for 1:1 ionic species.[31] The parameter ρ is the ratio of the solvent (water) density to its molecular weight; $\rho \approx 55.6$ mol L^{-1}. In this case, the standard free energy changes at low and high PDDA concentrations were estimated to be -54.3 and -40.8 kJ mol^{-1}, respectively. By way of comparison, the standard free energy change for adsorption of Chitosan into montmorillonite was estimated to be -55.6 kJ mol^{-1},[22a] and the constant value obtained indicates that the conformation of Chitosan does not change with W. In the case of PDDA, we can attribute the two different slopes to different conformations of the polymer as illustrated in Scheme 1. PDDA is extended at low PDDA concentration, as is the case with the Chitosan. The similar free energies of adsorption of PDDA and Chitosan indicate strong adsorption of PDDA on the clay interlayer surface through electrostatic interactions at low loading. The two distinct ΔG°_{ads} values for PDDA intercalation indicate different adsorption states of PDDA in the clay interlayer. Assuming PDDA is a strong electrolyte and fully dissociates in aqueous solution, the maximum amount adsorbed in Na-TSM should be equal to the CEC, which is 1.2 mequiv/g. The actual adsorbed amount of PDDA was lower than the CEC before the inflection point of the Scatchard plot. After the inflection point, the adsorbed amount of PDDA surpasses the CEC and approaches $W_s = 1.72$ mequiv/g (Figure 4). This indicates the adsorption of excess cationic polymer, along with Cl^- counterions that can be exchanged for other anionic guest molecules. This structural model (see Scheme 1) is also consistent with the progressive increase in the interlayer spacing with increasing PDDA concentration (Figure 2).

When we studied the intercalation of PDDA into a synthetic fluoromica with low CEC (45 mequiv/100 g clay, abbreviated as Na-TSM(L)),[32] the interlayer spacing did not change with increasing PDDA concentration as it did with Na-TSM. This indicates that the PDDA chain does not coil up (reaction 2 in Scheme 1) in the low charge density environment even at high solution concentration of PDDA. With the low charge density host Na-TSM(L), the layer charge is more easily compensated with PDDA in its extended conformation, and therefore there is less driving force to intercalate additional PDDA. Attempts to intercalate B1 into PDDA/Na-TSM(L) resulted in only a small uptake (2.02 mmol/100 g Na-TSM(L)) and no significant change in the XRD pattern. In contrast, with Na-TSM, some coiling of PDDA molecules is needed to match the higher charge density of the sheets. This model also explains why PEI and PAH intercalate as monolayers into Na-TSM at low pH, where their charge density is higher and better matches the charge density of the sheets. PAH shows evidence of coiling at high pH, where it has lower charge density, as illustrated in Figure 2.

(28) Giles, C. H.; MacEwan, T. H.; Nakhwa, S. N.; Smith, D. *J. Chem. Soc.* **1960**, 3973−3993.
(29) Langmuir, I. *J. Am. Chem. Soc.* **1916**, *38*, 2221−2295.
(30) Steinhardt, J.; Reynols, J. A. *Multiple Equilibria in Proteins*; Academic Press: New York, 1969.
(31) Miller, R.; Fainerman, V. B.; Möhwald, H. *J. Colloid Interface Sci.* **2002**, *247*, 193−199.
(32) Na-TSM with low CEC was available from Topy Ind. Co.

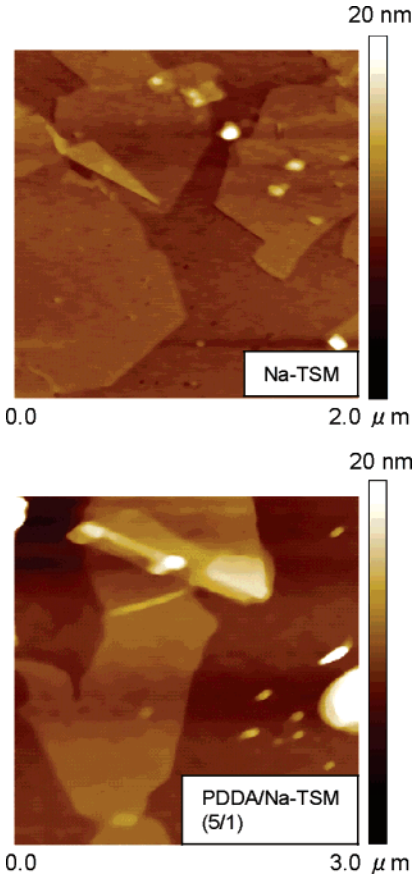

Figure 5. Tapping mode AFM images of delaminated Na-TSM and PDDA/Na-TSM (10/1) sheets deposited on a Si wafer functionalized sequentially with PDDA and PSS.

Morphology of the PDDA/Na-TSM Nanocomposites. To produce a cationic layered host of general utility for anion intercalation, it is important to maintain the morphology of the nanosheets. Figure 5 shows tapping mode atomic force microscopy (AFM) images of Na-TSM and PDDA/Na-TSM (10/1) sheets deposited on a PDDA-PSS functionalized Si wafer. This adsorption process may select the smallest particles in the suspension, and the observation of individual sheets does not therefore mean that the clay remains completely exfoliated in the presence of excess PDDA. Nevertheless, it is clear that the sheets imaged retain their two-dimensional morphology even after the adsorption of PDDA at high concentration. Height profile scans of PDDA/Na-TSM (10/1) indicated a flat plateau of 2.00 ± 0.24 nm average height, based on a 20 point cross-section of the AFM image. The average height of Na-TSM sheets measured before intercalation was 1.24 ± 0.18 nm, corresponding to an increase of 0.76 nm upon intercalation of PDDA. This value is in good agreement with the difference in *d*-spacings observed by XRD (0.77 nm).

Attempts were made to obtain AFM images of PDDA/Na-TSM (1/1) in the same manner. However, very few particles adhered to the (negatively charged) PSS/PDDA/Si substrate. For PDDA/Na-TSM (1/1), the amount of PDDA adsorbed was about 81% of the CEC of Na-TSM, implying that the net surface charge of the particles should be negative in dilute aqueous suspensions. This observation supports the idea that sheets of the 10/1 sample are indeed deposited electrostatically as cationic colloidal particles onto the PSS-terminated surface.

Encapsulation of the Anionic Dye Molecule B1 by PDDA/Na-TSM. To investigate the anion exchange behavior of the polycation/Na-TSM nanocomposites, the intercalation of an acidic dye, FD & C Blue No. 1 (Figure 1), was studied. Only a small amount of B1 (0.50 mmol/100 g Na-TSM) adsorbs in the absence of intercalated polycations. Also, the unexpandable host K-FM, even in the presence of PDDA, adsorbed only 0.57 mmol/100 g of the B1 dye. The polymer (PEI, PAH, and PDDA)/Na-TSM composites were all effective in intercalating 10−30 times this amount of the anionic dye, although in the case of PEI and PAH the adsorption was pH dependent, and intermolecular acid−base interactions (as evidenced by color changes) were apparently an important driving force for the intercalation reaction. The PDDA/Na-TSM composites intercalated B1 with retention of the blue color of the dye, and the reaction was independent of pH. B1/PDDA/Na-TSM is thus itself an interesting lamellar blue pigment that may have useful applications.

Flocculation of PDDA/Na-TSM occurred upon reaction with the B1 dye, even though the original nanocomposite was quite well dispersed in water. We tentatively attribute this behavior to the increased hydrophobicity of the material when the hydrophobic dye is added.

XRD and Elemental Analysis of Dye-Loaded PDDA/Na-TSM. Figure 6 shows XRD patterns of samples with different loadings of PDDA before and after the reaction with anionic dye B1. Analytical data for the dye loaded composites are summarized in Table 1. The amount of B1 intercalated was calculated from the difference in carbon content before and after the reaction.

In the XRD patterns of B1/PDDA/Na-TSM = 1/1/1 and 1/2/1, prominent shoulders at $d \approx 2.00$ nm were observed on the low angle side of the principal diffraction peak of PDDA/Na-TSM, indicating the presence of a new intercalated phase. The difference in peak positions was 0.48 nm in each case, but the low angle peak was larger in the (1/2/1) case, consistent with a larger proportion of the B1-containing phase. The remnant peaks at $d \approx 1.50$ nm suggest that a significant fraction of the PDDA/Na-TSM sample encapsulates very few B1 molecules. For the B1/PDDA/Na-TSM (1/1/1) and (1/2/1) samples, the mole ratios of PDDA to the CEC of Na-TSM were 0.78 and 1.02, respectively. These samples nevertheless adsorbed significant quantities (5.00 and 9.11 mmol/100 g Na-TSM, respectively) of B1.

In the case of the (1/3/1) and (1/5/1) samples, the *d*-spacings of the PDDA/Na-TSM starting materials were 1.77 and 1.84 nm, respectively. Interestingly, reaction with B1 again gives two product phases, but with taller and shorter gallery heights than the starting material. The difference in lattice spacing between the two phases after B1 intercalation was 0.72 nm in both cases, consistent with the larger amount of B1 incorporated (see Table 1) than in the (1/1/1) and (1/2/1) cases. With the 1/10/1 sample, there are again two product phases. This sample incorporates the most B1 dye, and the two product phases have a gallery height difference of 1.05 nm.

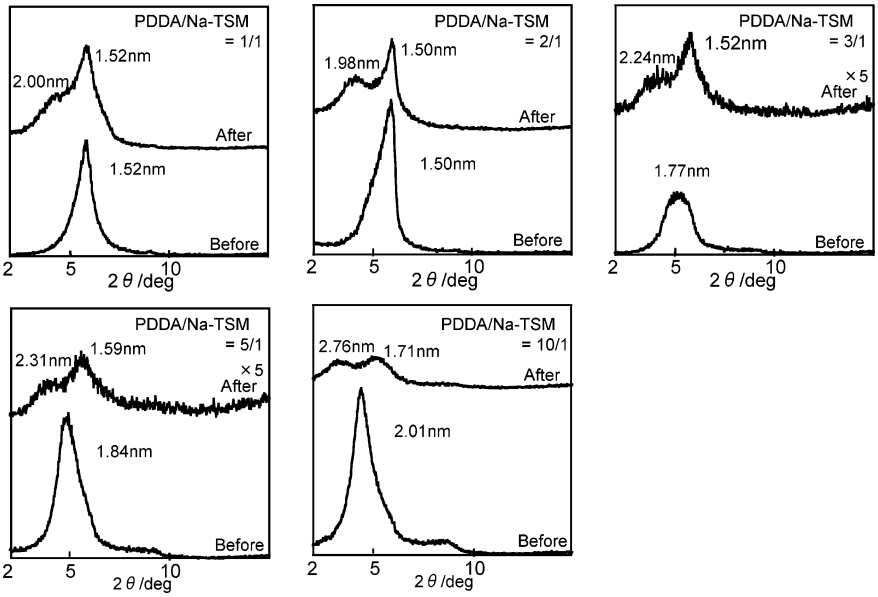

Figure 6. XRD patterns of PDDA/Na-TSM before and after intercalation of B1; PDDA/Na-TSM = 1/1, 2/1, 3/1, 5/1, and 10/1.

There are several possible explanations for the observation of two product phases in each B1/PDDA/Na-TSM nanocomposite. One is that the reaction does not reach equilibrium because of kinetic limitations, and that some residual PDDA/Na-TSM remains. However, this hypothesis is not consistent with the formation of products with shorter gallery heights in the (1/3/1), (1/5/1), and (1/10/1) cases. Another possible explanation is that the reaction with B1 may result in release of PDDA from the interlayers. It is well known that polycations such as PDDA can act as flocculating agent for nanoparticles, and this can actually be a sensitive test for release of polycations into solution. When a transparent suspension of laponite clay, which has a primary sheet size of 20 nm × 1 nm, was added to the supernatant after adsorption of B1, no flocculation was observed. In a control experiment, flocculation was observed when laponite was added to a PDDA solution at a concentration corresponding to release of 5% of the PDDA from B1/PDDA/Na-TSM (1/10/1). Therefore, we can eliminate the possibility that significant amounts of PDDA desorb during intercalation of B1. A third explanation is that two chemically distinct kinds of layers exist in each PDDA/Na-TSM composite, one type being more easily intercalated (by virtue of lower or higher charge density) by B1 than the other. Final explanation is that the B1-intercalated material spontaneously separates into two phases, in a manner that is analogous to staging in graphite intercalation compounds. A model for this kind of microscopic phase separation is shown in Scheme 2.

Yang et al. reported that Na-TSM, which is made from talc and Na_2SiF_6, has two kinds of layers with different charge densities; one type of layer has 0.37 e^-/Si_4O_{10}, and the other has 0.28 e^-/Si_4O_{10}.[26c] On the basis of intercalation experiments with *n*-alkylammonium cations, Yang et al. concluded from X-ray powder diffraction data and a computer simulation that these two kinds of interlayers are ordered along the *c*-axis in an ABABAB... sequence.[26c] We do not observe superlattice peaks that would support such an ordered structure in the B1/PDDA/Na-TSM or PDDA/Na-TSM materials. A stacking sequence consisting of locally segregated (AAAA... and BBBB...) high and low charge density phases could explain several of our observations. However, it seems unlikely that the fully exfoliated Na-TSM sheets would restack during the centrifugation and drying processes in such an ordered manner when intercalated with PDDA.

Scheme 2. Structural Model for a Na-TSM Nanocomposite Particle Containing Two Microscopically Separated Phases[a]

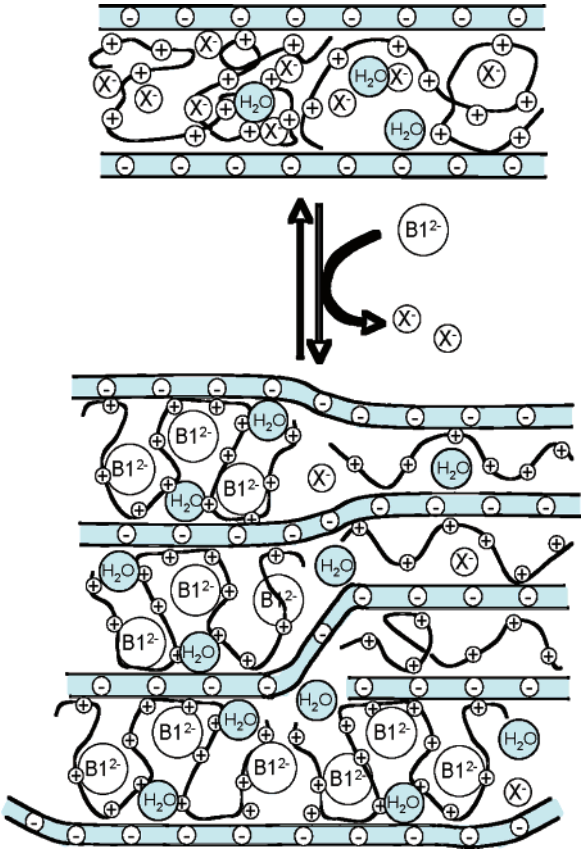

[a] The two phases contain hydrated B1/coiled PDDA and largely anhydrous uncoiled PDDA, respectively.

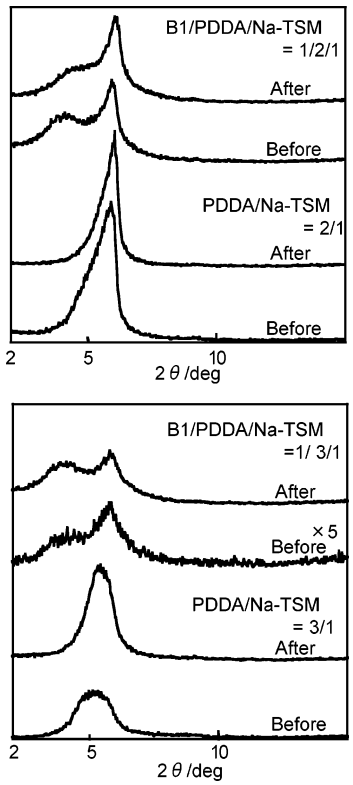

Figure 7. XRD patterns of PDDA/Na-TSM = 2/1 and B1/PDDA/Na-TSM = 1/2/1, and PDDA/Na-TSM = 3/1 and B1/PDDA/Na-TSM = 1/3/1, before and after dehydration at 392 K for 24 h.

To further investigate the structure of the two phases seen in the B1/PDDA/Na-TSM and PDDA/Na-TSM nanocomposites, a series of dehydration experiments were carried out. As noted above, water within the interlayers of Na-TSM can be eliminated by heating at 393 K for 24 h, resulting in a decrease in the layer spacing. As representative examples, the XRD patterns of B1/PDDA/Na-TSMs (1/2/1 and 1/3/1) and PDDA/Na-TSMs (2/1 and 3/1) are shown before and after dehydration in Figure 7. Dehydration of PDDA/Na-TSM (2/1) changes the shape but not the position of the maximum of the diffraction peak at 1.5 nm. The diffraction intensity on the low angle side of this asymmetric peak decreases, indicating that some of the galleries that originally contained water molecules collapsed to resemble the anhydrous PDDA-intercalated galleries. In contrast, in the case of PDDA/Na-TSM (3/1), which contains a coiled intercalated polymer layer, the entire peak shifts to higher angle, meaning that most or all of the galleries were initially hydrated. In the XRD patterns of B1/PDDA/Na-TSMs (1/2/1 and 1/3/1) before and after dehydration, higher angle peaks ($d = 1.50-1.52$ nm) that correspond to an intercalated PDDA monolayer with little intercalated B1 do not shift significantly, whereas the B1 intercalated phase collapses by 0.2−0.3 nm. This indicates that the phase containing B1 is hydrated, whereas the other phase is largely anhydrous, as illustrated in Scheme 2.

These results suggest that the reason for the appearance of two layer lines in the (3/1), (5/1), and (10/1) XRD patterns in Figure 6 is phase separation into a hydrated B1-PDDA intercalated phase, and more compact and anhydrous phase containing a largely uncoiled layer of PDDA. This phase may be driven by the favorable lattice energy of the compact PDDA-intercalated phase, just as staging in graphite intercalation reactions is driven by the favorable van der Waals energy of contacting carbon sheets. Interestingly, the B1 intercalation reaction appears to involve transfer of some PDDA to the B1-intercalated galleries, because the layer spacing in the more collapsed product phase is lower than that of the PDDA/Na-TSM starting material. This can occur easily if both microphases exist within the same particle, as illustrated in Scheme 2.

Spectroscopic Analysis (FT-IR and UV−Vis). In the FT-IR spectrum of B1/PDDA/Na-TSM (1/5/1), the typical bands due to B1 were observed in addition to the typical ones of Na-TSM and PDDA, indicating the combination of B1 and PDDA/Na-TSM (see Supporting Information). The antisymmetric stretching band attributed to sulfonate groups of B1 shifted from 1168 to 1192 cm^{-1} after the intercalation reaction. This shift may arise from the more hydrophobic environment of the intercalated phase and/or from the difference in specific electrostatic interactions between the sulfonate group and cations in the two environments (the B1 salt and the intercalation compound). Spectra of all of the B1/PDDA/Na-TSM composites with different loadings of PDDA were similar to each other, with no observable differences υ_{as} of $S(=O)_2$ or other specific bands. This indicates that the environment of B1 is similar in all of the B1/PDDA/Na-TSM nanocomposites.

Table 2 shows UV−visible absorption maxima of a 1 mM B1 aqueous solution, a 1:1 mixture solution of B1 (0.5 mM) and PDDA (0.5 mM), and 0.02 wt % suspensions of B1/PDDA/Na-TSM (1/1/1), (1/3/1), (1/5/1), and (1/10/1) (see Supporting Information for spectra). Because both B1 and PDDA are strong electrolytes, there is little interaction between the quaternary ammonium groups of PDDA and the anionic sulfonate groups of B1 in dilute aqueous solutions, and therefore the λ_{max} value does not change with addition of PDDA. In contrast, λ_{max} shifts progressively to the red with increasing PDDA content in the B1/PDDA/Na-TSM nanocomposites. There have been many reports concerning bathochromic spectral shifts, which depend on the aggregation and adsorption state of dyes on the internal or external surfaces of host materials.[4,33−36] With clay−porphyrin nanocomposites, the bathochromic shift of the porphyrin Soret band depends on the degree of flattening of the chromophore and the nature of the adsorption site (on the surface or in the interlayer).[35,36] From the XRD patterns, in B1/PDDA/Na-TSM (1/1/1 and 1/2/1), the change in gallery height upon intercalation (0.48 nm) suggests that the B1 molecules may be oriented parallel to the sheets. At higher PDDA loading (1/3/1 to 1/10/1), the galllery heights are larger than the dimensions of the molecule, and one cannot therefore draw conclusions about the orientation of B1. We tentatively attribute the bathochromic shift in this system to the increasingly hydrophobic character of the local

(33) (a) Ogawa, M. *Chem. Mater.* **1996**, *8*, 1347−1349. (b) Ogawa, M.; Kawai, R.; Kuroda, K. *J. Phys. Chem.* **1996**, *100*, 16218−16221.
(34) Kuykendall, V. G.; Thomas, J. K. *Langmuir* **1990**, *6*, 1350−1356.
(35) Chernia, Z.; Gill, D. *Langmuir* **1999**, *15*, 1625−1633.
(36) Takagi, S.; Shimada, T.; Eguchi, M.; Yui, T.; Yoshida, H.; Tryk, D. A.; Inoue, H. *Langmuir* **2002**, *18*, 2265−2272.

Table 2. Absorbance Maxima for the B1 Dye in Solution and in B1/PDDA/Na-TSM

	aqueous solution		B1/PDDA/Na-TSM nanocomposite				
	B1	1/1 mixture of B1 and PDDA	1/1/1	1/2/1	1/3/1	1/5/1	1/10/1
λ_{max}/nm	626	627	638	638	648	654	658

environment with increasing PDDA content in the host material.

Conclusions

The intercalation of three kinds of cationic polyelectrolytes (PEI, PAH, and PDDA) into a synthetic Na-fluoromica was studied as a means of inverting the layer charge and making a lamellar nanocomposite that could accommodate bulky anionic guests. In the case of PEI and PAH, the polycation conformation in the intercalated phase was pH dependent. At low pH and to some extent at high pH, these polymers tended to form monolayer intercalation compounds in which the polymer adopted an extended rather than coiled conformation. In contrast, with PDDA a coiled conformation that overcompensated the layer charge was obtained at higher polymer concentrations. The difference between PDDA and PEI or PAH appears to derive from the fact that the layer charged density is better matched by the latter polymers in their extended conformations, and therefore coiling is not required to compensate the charge on the sheets. The Scatchard plot showed clear evidence for different free energies of adsorption of PDDA in the extended and coiled conformations, and the transition between the two was consistent with layer spacings measured by X-ray diffraction.

The intercalation of anionic dye B1 into PDDA/Na-TSM occurs preferentially with nanocomposites that contain the coiled PDDA phase. Interestingly, this reaction drives the phase separation of the nanocomposite into a B1-rich phase containing coiled PDDA and a B1-poor phase containing predominantly extended PDDA. These experiments suggest that lamellar cation exchangers of slightly higher and/or more uniform charge density should be very interesting hosts for coiled polycations that could accommodate anionic guest molecules. While the focus in this work has been to prepare a lamellar dye nanocomposite that might be of interest in applications such as pigments and cosmetics, we note that there are many other possible uses for anion intercalators. For example, low charge density anions such as ClO_4^- and TcO_4^- are of concern as environmental contaminants, and selective sorbents for these anions are needed. Anionic dye molecules are also interesting for applications in artificial photosynthesis, photodynamic therapy, and biomedical imaging. The availability of nanocomposite hosts for low charge density anions is thus a significant step toward these applications.

Acknowledgment. This paper is dedicated to Professor Neil Bartlett on the occasion of his 75th birthday. This research was supported by the National Science Foundation under grant CHE-0616450. H.H. thanks Shiseido Co. Ltd. for giving him the opportunity to study at The Pennsylvania State University and for financial support.

Supporting Information Available: FT-IR spectra of B1, PDDA/Na-TSM (5/1), and B1/PDDA/Na-TSM (1/5/1) and UV−vis absorption spectra of a B1 aqueous solution, a 1:1 mixture solution of B1 and PDDA, and suspensions of B1/PDDA/Na-TSM (1/1/1), (1/3/1), (1/5/1), and (1/10/1) (PDF). This material is available free of charge via the Internet at http://pubs.acs.org.

CM061908C